

Complexes with Platinum–Ruthenium Bonds: The Stepwise Formation of Complexes Containing PtRu and PtRu₂ Units

Brian T. Sterenberg, Michael C. Jennings, and Richard J. Puddephatt*

Department of Chemistry, University of Western Ontario, London, Ontario, Canada N6A 5B7

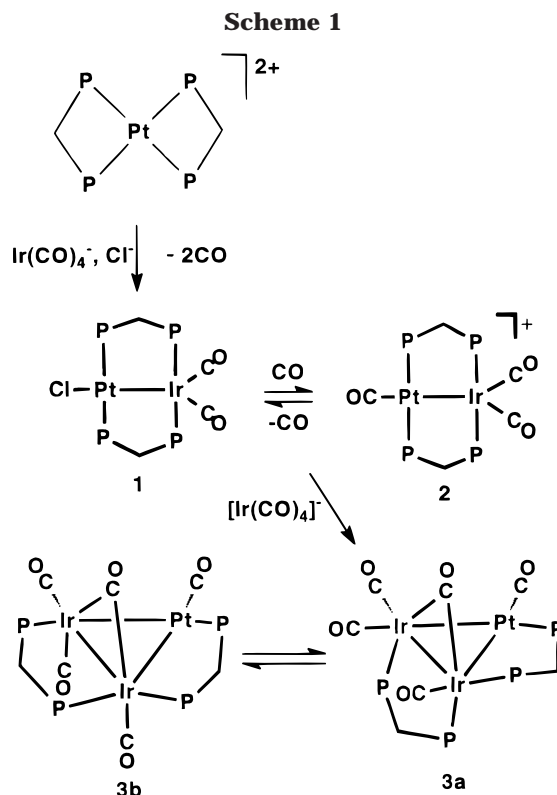
Received January 20, 1999

The reaction of $[\text{Pt}(\text{dppm})_2]\text{Cl}_2$, $\text{dppm} = \text{Ph}_2\text{PCH}_2\text{PPh}_2$, with $[\text{HRu}(\text{CO})_4]^-$ in a 1:2 ratio leads in a multistep reaction to the new heteronuclear cluster $[\text{PtRu}_2(\text{CO})_5(\mu\text{-CO})(\mu\text{-dppm})_2]$, which contains a triangle of metal atoms having both Pt–Ru edges bridged by dppm ligands. The initial step in the reaction is the formation of the heterobimetallic complex $[\text{PtRuH}(\text{CO})_3(\mu\text{-dppm})_2]^+$, which then reacts with additional $[\text{HRu}(\text{CO})_4]^-$ to form the PtRu₂ cluster. In the absence of excess $[\text{HRu}(\text{CO})_4]^-$, the complex $[\text{PtRuH}(\text{CO})_3(\mu\text{-dppm})_2]^+$ undergoes chloride for carbonyl substitution at ruthenium to give $[\text{PtRuHCl}(\text{CO})(\mu\text{-CO})(\mu\text{-dppm})_2]$. This complex then reacts further with chlorinated solvent to give $[\text{PtRu}(\text{Cl})_2(\text{CO})_2(\mu\text{-dppm})_2]$, which exists in two isomeric forms, one of which contains a semibridging carbonyl ligand. The structures of $[\text{PtRu}_2(\text{CO})_5(\mu\text{-CO})(\mu\text{-dppm})_2]$ and one isomer of $[\text{PtRu}(\text{Cl})_2(\text{CO})_2(\mu\text{-dppm})_2]$ have been determined crystallographically.

Introduction

Mixed metal cluster complexes of platinum have received considerable attention due to their potential to act as models for mixed metal catalysts.¹ Platinum–ruthenium bonded clusters are of particular interest because supported Pt/Ru/alumina catalysts are useful in petroleum refining and platinum–ruthenium electrodes are used to catalyze methanol oxidation in fuel cells.² Platinum–ruthenium clusters themselves have also been shown to be catalysts for hydrogenation and hydrosilylation of alkynes.³

The ability of many different metals, including main group metals such as tin, mid-transition metals such as rhenium, and several group 8–10 metals such as ruthenium or iridium to enhance the utility of platinum catalysts is remarkable and prompted a research program on the planned synthesis of complexes containing Pt–M bonds and studies of their reactivity.⁴ It was shown recently that complexes containing PtIr (**1** and **2**) and PtIr₂ (**3a** and **3b**) units could be formed by the stepwise addition of $[\text{Ir}(\text{CO})_4]^-$ to $[\text{Pt}(\text{dppm})_2]^{2+}$ as shown in Scheme 1.⁵ This paper reports the analogous formation of PtRu and PtRu₂ bonded clusters by reaction of $[\text{HRu}(\text{CO})_4]^-$ with $[\text{Pt}(\text{dppm})_2]^{2+}$. Although several mixed metal clusters of the form PtRu₂ are known,



(1) (a) Farrugia, L. J. *Adv. Organomet. Chem.* **1990**, *31*, 301. (b) *The Chemistry of Heteronuclear Clusters and Multimetallic Catalysts*; Adams, R. D., Herrmann, W. A., Eds.; *Polyhedron* **1988**, *7*, 2251–2462. (c) *Comprehensive Organometallic Chemistry II*; Abel, E. W., Stone, F. G. A., Wilkinson, G., Eds.; *Heteronuclear Metal–Metal Bonds*, Vol. 10; Adams, R. D., Ed.; Elsevier: Oxford, 1995.

(2) (a) Miura, H.; Taguchi, H.; Sugiyama, K.; Matsuda, T.; Gonzalez, R. D. *J. Catal.* **1990**, *124*, 194. (b) Lee, C. E.; Bergens, S. H. *J. Phys. Chem. B* **1998**, *102*, 193.

(3) (a) Adams, R. D.; Barnard, T. S.; Li, Z. Y.; Wu, W. G.; Yamamoto, J. H. *J. Am. Chem. Soc.* **1994**, *116*, 9103. (b) Adams, R. D.; Barnard, T. S. *Organometallics* **1998**, *17*, 2567.

(4) Xiao, J.; Puddephatt, R. J. *Coord. Chem. Rev.* **1995**, *143*, 457.

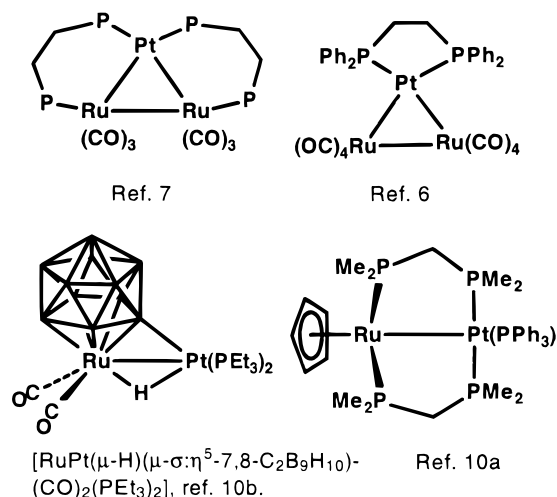
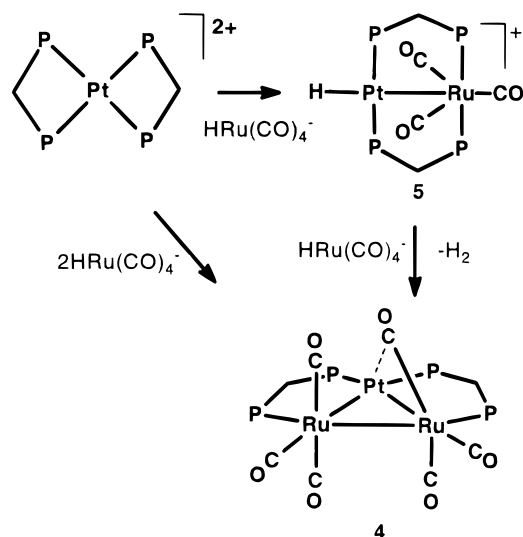
(5) Sterenberg, B. T.; Jenkins, H. A.; Puddephatt, R. J. *Organometallics*, in press.

simple routes to them are not common. Previously characterized examples include $[\text{PtRu}_2(\text{CO})_8(\text{dppe})]$,⁶ $[\text{PtRu}_2(\text{CO})_6(\text{dppe})_2]$,⁷ $[\text{Ru}_2\text{Pt}(\text{CO})_5(\text{CNBu}^t)(\text{PPh}_3)_4]$,⁸ and $[\text{PtRu}_2(\mu\text{-PPh}_2)(\mu\text{-H})(\text{CO})_7(\text{PCy}_3)]$.⁹ These clusters were

(6) (a) Adams, R. D.; Chen, G.; Wang, J.; Wu, W. *Organometallics* **1990**, *9*, 1339. (b) Bruce, M. I.; Shaw, G.; Stone, F. G. A. *J. Chem. Soc., Dalton Trans.* **1972**, 1781.

(7) Adams, R. D.; Chen, G.; Wu, W. *J. Cluster Sci.* **1993**, *4*, 119.

(8) Bruce, M. I.; Matison, J. G.; Skelton, B. W.; White, A. H. *Aust. J. Chem.* **1982**, *35*, 687.

Chart 1. Known PtRu₂ and PtRu Bonded Complexes**Scheme 2**

either formed by degradation of a higher nuclearity cluster or isolated in low yield from mixtures containing other cluster complexes.^{6–9} Heterobimetallic complexes containing Pt–Ru bonds are surprisingly rare,¹⁰ and dppm-bridged PtRu complexes are unknown. Some of the known complexes containing PtRu or PtRu₂ units are shown in Chart 1.

Results and Discussion

Synthesis of the PtRu₂ Cluster [PtRu₂(CO)₅(μ-CO)(μ-dppm)₂], 4. By analogy with the known reactions of [Pt(dppm)₂]Cl₂ with [Ir(CO)₄][–] to give PtIr₂ clusters **3** (Scheme 1),⁵ the synthesis of PtRu₂ clusters by the reaction of [Pt(dppm)₂]²⁺ with [PPN][HRu(CO)₄][–] was studied. The reaction led to the complex [PtRu₂(CO)₅(μ-CO)(μ-dppm)₂], **4**, Scheme 2, which was isolated

Table 1. Crystal Data and Structure Refinement

	4	7a
formula	C ₅₆ H ₄₄ O ₆ P ₄ PtRu ₂	C _{55.5} H ₅₂ Cl ₄ O ₂ P ₄ PtRu
fw	334.02	1312.81
temp (K)	100(2)	292(2)
wavelength (Å)	0.710 73	0.710 73
space group	<i>P</i> 2 ₁ / <i>n</i>	Cc
<i>a</i> (Å)	12.444(3)	19.788(4)
<i>b</i> (Å)	16.842(3)	16.897(3)
<i>c</i> (Å)	23.757(5)	17.302(4)
β (deg)	96.19	106.37(3)
volume (Å ³)	4950(2)	5550.8(19)
<i>Z</i>	4	4
ρ (calc) (Mg/m ³)	1.790	1.571
abs coeff (mm ^{–1})	3.603	3.137
no. of ind reflns	10 042 (<i>R</i> _{int} = 0.0460)	5627 [<i>R</i> _{int} = 0.0940]
no. of data/ restraints/ params	10042/0/622	5627/9/608
G-o-F on <i>F</i> ²	1.059	1.047
<i>R</i> [<i>I</i> > 2σ(<i>I</i>)]	R1 0.0288	0.0497
	wR2 0.0621	0.1384
<i>R</i> (all data)	R1 0.0429	0.0526
	wR2 0.0667	0.1426

as an orange solid and characterized both spectroscopically and by an X-ray structure determination.

The ³¹P NMR spectrum of complex **4** contains two resonances at δ = 16.8 [d, ²*J*(PP) = 48 Hz, RuP] and 8.3 [d, ²*J*(PP) = 48 Hz, ¹*J*(PtP) = 3130 Hz, PtP] in a 1:1 ratio. The presence of only two resonances in the ³¹P spectrum indicates that the molecule **4** has an effective mirror plane which contains the Pt atom and bisects the Ru–Ru bond. Hence both dppm ligands bridge Pt–Ru edges of the PtRu₂ triangle and the Ru–Ru edge is not bridged. The structure thus differs from those of the analogous PtIr₂ clusters **3a** and **3b**, in which the dppm ligands bridge one Pt–Ir edge and the Ir–Ir edge, with one Pt–Ir edge unbridged. The ¹H NMR spectrum of **4** contains a single resonance at δ = 4.48 for the dppm methylene groups, indicating that there is an effective mirror plane containing the PtRu₂(PCP)₂ atoms. The spectrum contains no hydride resonance, and the stoichiometry of formation of **4** requires loss of the hydride ligands from the 2 equiv of the reagent [HRu(CO)₄][–] as dihydrogen. When the reaction was carried out in a sealed NMR tube, dihydrogen was positively identified by its ¹H NMR spectrum (δ = 4.6), thus supporting the proposed stoichiometry. The ¹³C NMR spectrum of **4** shows two carbonyl resonances in a 2:1 ratio for the four axial carbonyls and the two equatorial carbonyls, respectively. The resonance for the equatorial carbonyls shows a long-range coupling ³*J*(PPtRuC) = 21 Hz, which is consistent with the phosphorus and carbonyl being approximately collinear with the PtRu bond. The resonance for the axial carbonyls shows a coupling *J*(PtC) = 34 Hz, perhaps indicating a weak bridging of these carbonyls to platinum. However, the lowest carbonyl stretching frequency in the IR spectrum occurs at 1878 cm^{–1}, which suggests a weak semibridging interaction only.

The basic features of the structure of **4** deduced from the spectra were confirmed by the structure determination (Table 1). A view of the structure is shown in Figure 1, and selected bond lengths and angles are given in Table 2. The three metal atoms form a triangle, and the two Pt–Ru edges of the triangle are each bridged by a dppm ligand. The three metals and four phosphorus

(9) (a) Powell, J.; Brewer, J. C.; Gulia, G.; Sawyer, J. F. *Inorg. Chem.* **1989**, *28*, 4470–1650. (b) Kuwata, S.; Mizobe, Y.; Hidai, M. *J. Am. Chem. Soc.* **1993**, *115*, 8499.

(10) (a) Mague, J. T.; Balakrishna, M. S. *J. Organomet. Chem.* **1996**, *23*, 4259. (b) Anderson, S.; Mullica, D. F.; Sappenfield, E. L.; Stone, F. G. A. *Organometallics* **1995**, *14*, 3516. (c) Akabori, S.; Kumagai, T.; Shirahige, T. *Organometallics* **1987**, *6*, 526. (d) Powell, J.; Fuchs, E.; Gregg, M. R.; Phillips, J.; Stainer, M. V. R. *Organometallics* **1990**, *9*, 387.

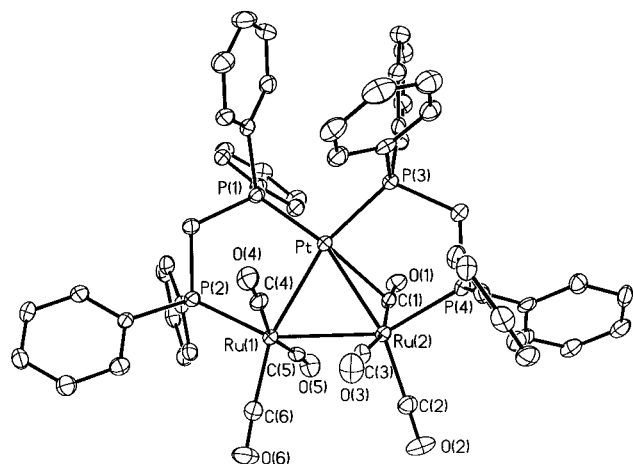


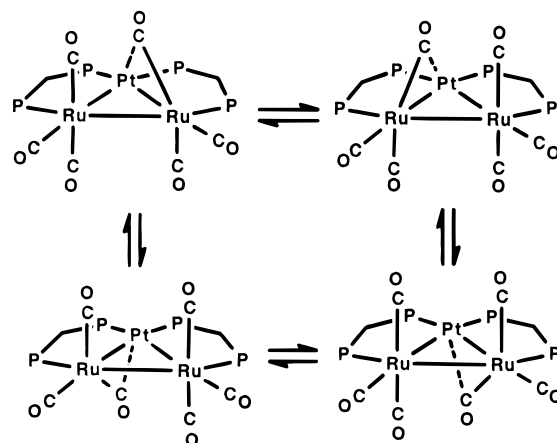
Figure 1. View of the structure of $[\text{PtRu}_2(\text{CO})_5(\mu\text{-CO})(\mu\text{-dppm})_2]$, **4**. Thermal ellipsoids are drawn at 30% probability. Hydrogen atoms have been omitted for clarity.

Table 2. Selected Bonds Lengths (Å) and Angles (deg) for $[\text{PtRu}_2(\text{CO})_5(\mu\text{-CO})(\mu\text{-dppm})_2]$, **4**

Pt–P(1)	2.255(1)	Ru(2)–C(1)	1.926(4)
Pt–P(3)	2.268(1)	Ru(2)–C(3)	1.940(5)
Pt–C(1)	2.534(4)	Ru(2)–P(4)	2.304(1)
Pt–Ru(1)	2.6757(6)	C(1)–O(1)	1.149(5)
Pt–Ru(2)	2.6793(9)	C(2)–O(2)	1.140(5)
Ru(1)–C(6)	1.906(5)	C(3)–O(3)	1.144(5)
Ru(1)–C(4)	1.915(4)	C(4)–O(4)	1.160(5)
Ru(1)–C(5)	1.928(4)	C(5)–O(5)	1.147(5)
Ru(1)–P(2)	2.318(1)	C(6)–O(6)	1.144(5)
Ru(1)–Ru(2)	2.8214(7)		
Ru(2)–C(2)	1.913(4)		
P(1)–Pt–P(3)	105.79(4)	C(6)–Ru(1)–C(5)	95.2(2)
P(1)–Pt–C(1)	128.5(1)	C(4)–Ru(1)–C(5)	163.0(2)
P(3)–Pt–C(1)	92.76(9)	C(6)–Ru(1)–P(2)	106.8(1)
P(1)–Pt–Ru(1)	94.63(4)	C(4)–Ru(1)–P(2)	88.5(1)
P(3)–Pt–Ru(1)	158.19(3)	C(5)–Ru(1)–P(2)	96.3(1)
C(1)–Pt–Ru(1)	80.03(9)	C(6)–Ru(1)–Pt	154.7(1)
P(1)–Pt–Ru(2)	156.51(3)	C(4)–Ru(1)–Pt	68.5(1)
P(3)–Pt–Ru(2)	97.11(3)	C(5)–Ru(1)–Pt	94.7(1)
C(1)–Pt–Ru(2)	43.3(1)	P(2)–Ru(1)–Pt	95.18(4)
Ru(1)–Pt–Ru(2)	63.59(2)	C(6)–Ru(1)–Ru(2)	100.5(1)
C(6)–Ru(1)–C(4)	99.1(2)	C(4)–Ru(1)–Ru(2)	87.0(1)
C(5)–Ru(1)–Ru(2)	81.2(1)	C(2)–Ru(2)–Ru(1)	104.5(1)
P(2)–Ru(1)–Ru(2)	152.74(3)	C(1)–Ru(2)–Ru(1)	87.7(1)
Pt–Ru(1)–Ru(2)	58.27(3)	C(3)–Ru(2)–Ru(1)	82.8(1)
C(2)–Ru(2)–C(1)	99.7(2)	P(4)–Ru(2)–Ru(1)	150.63(3)
C(2)–Ru(2)–C(3)	94.9(2)	Pt–Ru(2)–Ru(1)	58.14(2)
C(1)–Ru(2)–C(3)	164.2(2)	O(1)–C(1)–Ru(2)	173.8(3)
C(2)–Ru(2)–P(4)	104.8(1)	O(1)–C(1)–Pt	112.6(3)
C(3)–Ru(2)–P(4)	93.2(1)	Ru(2)–C(1)–Pt	72.4(1)
C(2)–Ru(2)–Pt	155.1(1)	O(2)–C(2)–Ru(2)	176.8(4)
C(1)–Ru(2)–Pt	64.3(1)	O(3)–C(3)–Ru(2)	176.4(4)
C(3)–Ru(2)–Pt	99.9(1)	O(4)–C(4)–Ru(1)	175.7(4)
P(4)–Ru(2)–Pt	94.33(3)	O(5)–C(5)–Ru(1)	177.1(3)
		O(6)–C(6)–Ru(1)	176.0(4)

atoms are approximately coplanar. The two Pt–Ru distances are very similar at 2.6757(6) and 2.6793(9) Å, while the unbridged Ru–Ru distance is significantly longer at 2.8214(7) Å. There are three carbonyl ligands on each ruthenium atom, which naturally gives a 16-electron configuration at platinum and an 18-electron configuration at each ruthenium. On Ru(1), all three carbonyls are terminal but one of the carbonyl ligands on Ru(2) forms a weak semibridging interaction to platinum. The Pt–C(1) distance is 2.534(4) Å, while the Ru(2)–C(1) distance is 1.926(4) Å, and the angles Pt–C(1)–O(1) (112.6(3)°) and Ru(2)–C(1)–O(1) (173.8(3)°) clearly show that the carbonyl is best considered as

Scheme 3

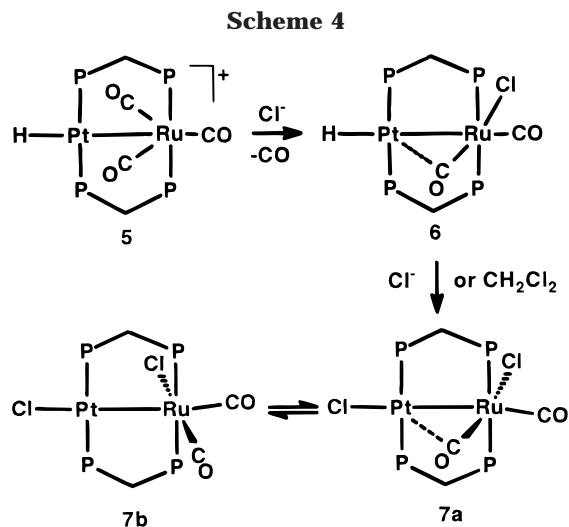


weakly semibridging. The semibridging interaction of the carbonyl on Ru(2) results in a deformation of the other carbonyl ligands, with the result that the carbonyl ligands on the two ruthenium atoms are in a staggered rather than eclipsed conformation (Figure 1).

The presence of a single semibridging carbonyl in the solid-state structure leads to overall C_s symmetry for the complex. This is clearly inconsistent with the C_{2v} symmetry in solution deduced from the NMR spectra. The apparent symmetry in solution results from a fluxional process in which the four axial carbonyl ligands exchange between terminal and weakly semibridging bonding modes, as shown in Scheme 3. Attempts were made to freeze out the fluxional process using variable-temperature NMR, but it is still fast on the NMR time scale even at -90°C . From examination of the structure in Figure 1, it is clear that only a very small movement of the carbonyls is required for this equilibration.

The Mechanism of Cluster Formation. The mechanism of formation of **4** clearly requires the addition of 2 equiv of $[\text{HRu}(\text{CO})_4]^-$ to $[\text{Pt}(\text{dppm})_2]^{2+}$, with loss of $\text{H}_2 + 2\text{CO}$. Attempts were made to observe intermediate complexes in this overall reaction by monitoring the reaction by NMR under varying conditions. Only the bimetallic intermediate complex $[\text{HPtRu}(\text{CO})_3(\mu\text{-dppm})_2]^+$, **5**, Scheme 2, was detected in this way. Compound **5** can be synthesized by reaction of $[\text{Pt}(\text{dppm})_2]\text{Cl}_2$ with 1 equiv of $\text{PPN}[\text{HRu}(\text{CO})_4]$ at low temperature, but it is difficult to purify, as discussed below, and so was characterized by its spectroscopic data.

The ^1H NMR spectrum of **5** shows a hydride peak at $\delta = -3.95$ [t, $^2J(\text{PH}) = 10$ Hz, $^1J(\text{PtH}) = 1270$ Hz], clearly indicating the presence of a terminal Pt–H group. The dppm methylene hydrogens appear as a single resonance at $\delta = 4.34$, indicating that there is a mirror plane containing the two metal and four phosphorus atoms. The ^{31}P NMR spectrum of **5** shows two multiplet resonances characteristic of an AA'XX' spin system at $\delta = 36.8$ [RuP] and 24.0 [$^1J(\text{PtP}) = 3260$ Hz, PtP], clearly showing that the dppm ligands bridge the PtRu unit. In the ^{13}C NMR spectrum of **5**, two resonances are observed at $\delta = 195.5$ [equatorial CO] and 207.8 [axial CO] in a 1:2 ratio, neither showing resolved $J(\text{PtC})$ coupling. The IR spectrum shows three terminal bands at 2042, 1988, and 1970 cm^{-1} . The structure can thus be unambiguously assigned as having a terminal



hydride on platinum, three terminal carbonyls on ruthenium, and a chloride counterion, as shown in Scheme 2. This structure therefore contains a 16-electron platinum center and an 18-electron ruthenium center. If the Pt–Ru bond is considered as a single covalent bond, the formal oxidation states are Pt(I)Ru(I), but it is also possible to consider this as a ruthenium to platinum donor–acceptor bond, and then the formal oxidation states are Pt(II)Ru(0).

The overall reaction leading to formation of cluster **4** is then suggested to occur as follows. The initial step is combination of the first equivalent of $\text{HRu}(\text{CO})_4^-$ and $[\text{Pt}(\text{dppm})_2]^{2+}$ to form $[\text{PtRuH}(\text{CO})_3(\mu\text{-dppm})_2]\text{Cl}$, **5**. This reaction occurs by nucleophilic attack of $[\text{HRu}(\text{CO})_4]^-$ on **1**, with rearrangement of the dppm ligands from chelating to bridging coordination, migration of hydride from ruthenium to platinum, and with loss of 1 equiv of CO. The next step is attack on the bimetallic complex **5** by the second equivalent of $[\text{HRu}(\text{CO})_4]^-$ with loss of H_2 and CO, to form the trimetallic cluster **4**. The initial attack by the second equivalent of $[\text{HRu}(\text{CO})_4]^-$ on **5** might be expected to occur at the 16-electron platinum center, but that should lead to insertion of ruthenium into a Pt–P bond and hence to formation of a $\text{Ru}_2(\mu\text{-dppm})$ edge, whereas the structure of **4** clearly requires insertion into a Ru–P bond and suggests attack by $[\text{HRu}(\text{CO})_4]^-$ at the ruthenium center of **5** with loss of CO. Migration of hydride from ruthenium to platinum followed by reductive elimination of H_2 would then lead to formation of **4**.

Further Chemistry of the Heterobimetallic Complex 5. Attempts to prepare complex **5** in pure form led instead to the isolation of two new PtRu bonded complexes, $[\text{PtRuHCl}(\text{CO})(\mu\text{-CO})(\mu\text{-dppm})_2]$, **6**, and $[\text{PtRuCl}_2(\text{CO})_2(\mu\text{-dppm})_2]$, **7**. The compound $[\text{PtRuHCl}(\text{CO})(\mu\text{-CO})(\mu\text{-dppm})_2]$, **6**, is formed from **5** by displacement of one carbonyl ligand by the chloride counterion as shown in Scheme 4. It is formed as the main product if the reaction of $\text{PPN}[\text{HRu}(\text{CO})_4]$ and $[\text{Pt}(\text{dppm})_2][\text{Cl}]_2$ is carried out in tetrahydrofuran solvent at room temperature and if the $\text{PPN}[\text{HRu}(\text{CO})_4]$ is added in a dropwise fashion. Complex **6** could not be isolated in pure form (it could not be separated from some impurity of cluster **4**), but it was completely characterized in solution. Complex **7** is formed when the above reaction is carried out in solution in dichloromethane, and its

formation from **6** requires the overall replacement of the hydride by chloride (Scheme 4). Complex **6** is detected as an intermediate, and complete conversion to **7** takes about 3 days.

The ^1H NMR spectrum of **6** shows a hydride resonance at $\delta = -5.45$ [tt, $^2J(\text{PPtH}) = 16$ Hz, $^3J(\text{PRuPtH}) = 3$ Hz, $^1J(\text{PtH}) = 1050$ Hz], and the large value of $^1J(\text{PtH})$ proves the presence of a terminal PtH group. Two resonances are seen for the dppm methylene hydrogen atoms, indicating that there is no plane of symmetry containing the PtRu(PCP) $_2$ atoms and hence that the chloride is axial rather than equatorial on ruthenium. The ^{13}C NMR spectrum shows two resonances at $\delta = 207.7$ [terminal CO] and 225.1 [bridging CO]. Although the chemical shift at $\delta = 225.1$ suggests a bridging carbonyl, no $^1J(\text{PtC})$ coupling is observed, and it is possible that the chemical shift reflects a strongly semibridging carbonyl. The IR spectrum shows two bands at 1880 and 1770 cm^{-1} and so lends support to the proposal that a bridging carbonyl is present.

In the ^1H NMR spectrum of **7** there is no hydride resonance, but the spectra are otherwise similar to those of **6**. Thus, there are two resonances in the ^1H NMR spectrum due to the CH^aH^b protons of the dppm ligands, and the ^{31}P NMR spectrum shows two multiplets due to the RuP and PtP atoms. The ^{13}C NMR spectrum gives two resonances at $\delta = 208.0$ and 192.4, both in the usual range for terminal RuCO groups and which show small couplings $J(\text{PtC}) = 117$ and 180 Hz, respectively.

The IR spectrum of **7** shows unusual features. In either the solid state or solution, an analytically pure sample of **7** showed four carbonyl bands at 2025, 1945, 1905, and 1792 cm^{-1} , though **7** contains only two carbonyl ligands. The relative intensities of the bands changed between the solid and solution state, indicating that the extra bands result from a second isomer of **7**. The bands at 1905 and 1792 cm^{-1} are favored in the solid state and are assigned to isomer **7a**, and the low-frequency stretch at 1792 cm^{-1} indicates the presence of a bridging carbonyl in **7a**. The bands at 2025 and 1945 cm^{-1} are more prominent in the solution state and indicate that the second isomer, **7b**, has only terminal carbonyl ligands. Note that both carbonyl bands for **7b** are at higher energy than those of **7a**. This is reasonable since the semibridging carbonyl in **7a** is involved in back-bonding with platinum so the remaining terminal carbonyl on ruthenium also back-bonds more strongly than the carbonyls in **7a**. Although the IR spectra clearly indicate that two isomers are present in solution, the NMR spectra contain only one set of peaks even at -90 $^\circ\text{C}$, indicating that the interconversion of the two isomers is very fast on the NMR time scale but slow on the IR time scale. The resonance in the ^{13}C NMR spectrum at $\delta = 208.0$ can now be assigned to the carbonyl that is semibridging in **7a** but terminal in **7b**. Thus, it has a significantly higher chemical shift than the resonance at $\delta = 192$, which is assigned to the carbonyl which is terminally bonded in both isomers.

One isomer of complex **7** has been structurally characterized. A diagram of the structure is shown in Figure 2, and selected bond lengths and angles are shown in Table 3. Clearly, the structurally characterized isomer is **7a**, since it contains a bridging carbonyl ligand. Recall that **7a** is the isomer favored in the solid state. The

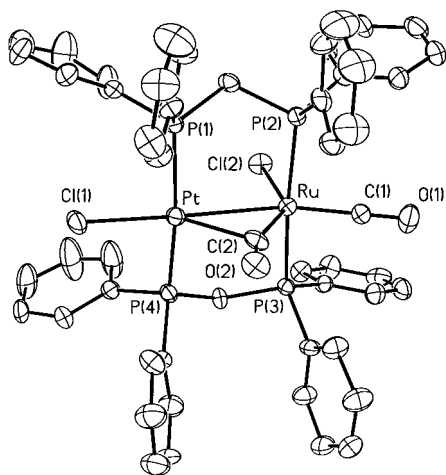


Figure 2. View of the structure of $[\text{PtRuCl}_2(\text{CO})(\mu\text{-CO})(\mu\text{-dppm})_2]$, **7a**. Thermal ellipsoids are drawn at 30% probability. Hydrogen atoms have been omitted for clarity.

Table 3. Selected Bond Lengths (Å) and Angles (deg) for $[\text{PtRuCl}_2(\text{CO})(\mu\text{-CO})(\mu\text{-dppm})_2]$ (7a**)**

Pt–C(2)	2.20(1)	Ru–C(2)	1.92(1)
Pt–P(4)	2.295(4)	Ru–P(2)	2.359(3)
Pt–P(1)	2.319(3)	Ru–P(3)	2.360(3)
Pt–Cl(1)	2.406(4)	Ru–Cl(2)	2.498(3)
Pt–Ru	2.823(1)	C(1)–O(1)	1.16(2)
Ru–C(1)	1.81(1)	C(2)–O(2)	1.15(2)
C(2)–Pt–P(4)	94.1(3)	C(1)–Ru–P(3)	88.3(5)
C(2)–Pt–P(1)	97.6(3)	C(2)–Ru–P(3)	93.1(4)
P(4)–Pt–P(1)	164.4(1)	P(2)–Ru–P(3)	169.9(1)
C(2)–Pt–Cl(1)	139.4(4)	C(1)–Ru–Cl(2)	113.3(6)
P(4)–Pt–Cl(1)	88.8(1)	C(2)–Ru–Cl(2)	141.4(4)
P(1)–Pt–Cl(1)	89.0(1)	P(2)–Ru–Cl(2)	85.5(1)
P(4)–Pt–Ru	91.5(1)	P(3)–Ru–Cl(2)	87.0(1)
P(1)–Pt–Ru	90.11(8)	C(1)–Ru–Pt	156.4(6)
Cl(1)–Pt–Ru	177.8(2)	P(2)–Ru–Pt	93.64(8)
C(1)–Ru–C(2)	105.3(7)	P(3)–Ru–Pt	93.24(8)
C(1)–Ru–P(2)	88.3(5)	Cl(2)–Ru–Pt	90.3(1)
C(2)–Ru–P(2)	97.0(4)		

structure of **7a** contains a *trans,trans*-PtRu(μ -dppm)₂ group with a metal–metal separation Pt–Ru = 2.823(1) Å, which is consistent with a single metal–metal bond, though the distance is longer than in most related complexes.^{6–10} For example, it is considerably longer than the Pt–Ru distances in cluster **4** (2.6757(6) and 2.6793(9) Å) and somewhat longer than in the binuclear complexes [PtRuCp(PPh₃)(Me₂PCH₂PMe₂)₂] (2.769(1) Å) and [PtRuH(μ - σ , η^5 -7,8-C₂B₉H₁₀)(CO)₂(PEt₃)₂] (2.802(1) Å).^{10a,b} In addition to the phosphine ligands, the ruthenium atom is bound to two carbonyl ligands and one chloride ligand, while the platinum atom is bound to one chloride and also forms a semibridging interaction with one of the ruthenium carbonyl ligands. This configuration results in an 18-electron Ru(I) center and a 16-electron Pt(I) center. The geometry at ruthenium is best considered as a highly distorted octahedron. The angles within the PtClP₂ unit are all close to 90°, so the stereochemistry at platinum is roughly square planar ignoring the semibridging carbonyl. The carbonyl ligand C(2)O(2) is bent toward the Pt atom to form the semibridging interaction. The angles Ru–C(2)–O(2) = 157(1)°, Pt–C(2)–O(2) = 116(1)° and distances Ru–C(2) = 1.92(1), Pt–C(2) = 2.20(1) Å clearly indicate a semibridging carbonyl. The terminal carbonyl C(1)O(1) is also bent from its ideal octahedral position *trans* to

the metal–metal bond such that the angle Pt–Ru–C(1) is 156.4(6)°, substantially less than 180°.

In the absence of structural characterization, the precise structure of the isomer **7b** must be deduced from the structure of **7a** and from the spectroscopic data. Clearly, the interconversion of the isomers is very facile so the difference in structures is probably minor. We suggest that formation of **7b** from **7a** occurs simply by breaking the semibridging Pt···CO interaction, thus allowing the ruthenium to adopt a more regular octahedral structure. In this way, the loss of the Pt···CO bonding component is balanced by the relief of angle strain at ruthenium, such that the isomers have similar energies. Interconversion between the isomers probably requires a change in conformation of the bridging dppm ligands, and this provides a small steric barrier since the ruthenium center is sterically crowded.

The structural characterization of **7a** clearly lends more support to the proposed structure of **6**. It is, however, interesting that the hydride–chloride complex **6** exists only in the bridging carbonyl form analogous to **7a**, with no evidence of a second isomer analogous to **7b**. The role of the semibridging carbonyl in **7a** is clearly to remove excess charge from platinum by back-bonding. Complex **6** contains the stronger electron-donating hydride ligand, which makes the platinum more electron rich and increases the strength of the semibridging carbonyl interaction. Hence, there is no equilibrium with the terminal carbonyl isomer analogous to **7b**.

Conclusions

The reaction of [RuH(CO)₄][–] with [Pt(dppm)₂]²⁺ occurs in a stepwise manner to give [PtRuH(CO)₃(μ -dppm)₂]⁺, **5**, and then [PtRu₂(CO)₆(μ -dppm)₂], **4**. Complex **5** acts as a precursor to the further Pt–Ru bonded complexes [PtRuHCl(CO)₂(μ -dppm)₂], **6**, and [PtRuCl₂(CO)₃(μ -dppm)₂], **7**. Reliable synthetic routes to these heterobimetallic Pt–Ru bonded complexes are particularly useful because there are few other examples of such complexes, which are the simplest models for the Pt/Ru surface chemistry that is important in bimetallic catalysis. A feature of both the binuclear Pt–Ru complexes, **6** and **7a**, and the PtRu₂ cluster complex, **4**, is the presence of semibridging carbonyl ligands, whose function appears to be to equalize the charge densities at the platinum and ruthenium centers by back-bonding of electron density away from the electron-rich platinum center.

Experimental Section

Infrared spectra were recorded as Nujol mulls using a Perkin-Elmer 2000 FTIR spectrometer. The ¹H, ³¹P{¹H}, and ¹³C{¹H} NMR spectra were recorded by using a Varian Gemini 300 NMR spectrometer. The compounds [PPN][Ir(CO)₄]⁺ and [Pt(dppm)₂]Cl₂⁵ were prepared by literature methods. All manipulations were carried out using standard Schlenk techniques under an atmosphere of prepurified argon except as indicated. Once formed, the pure Pt–Ru bonded complexes were only slowly decomposed by air.

[PtRu₂(CO)₅(μ -CO)(μ -dppm)₂] (4). [Pt(dppm)₂]Cl₂ (40 mg, 0.038 mmol) and excess PPN[HRu(CO)₄] (150 mg, 0.199 mmol) were cooled to –80 °C and dissolved in 30 mL of CH₂Cl₂ which

(11) Walker, H. W.; Ford, P. C. *J. Organomet. Chem.* **1981**, *214*, C43.

had been degassed with three freeze–pump–thaw cycles. The resulting red–orange solution was allowed to warm to room temperature and then stirred for 4 days. The solvent was removed in vacuo, and the residue was chromatographed on a silica gel column using CH_2Cl_2 as the eluent. The orange band was isolated, and the solvent was removed in vacuo. The residue was recrystallized from CH_2Cl_2 /pentane and dried in vacuo. Yield: 32 mg, 62%. Anal. Calcd for $\text{C}_{56}\text{H}_{44}\text{O}_6\text{P}_4\text{PtRu}_2$: C, 50.41; H, 3.32. Found: C, 50.29; H, 3.32. IR (Nujol): $\nu(\text{CO})$ 2007 (s), 1960 (s), 1940 (sh), 1924 (s), 1893 (s), 1878 (b). NMR in CD_2Cl_2 : $\delta(^1\text{H}) = 4.48$ [PCH₂P, m], $\delta(^{31}\text{P}) = 16.8$ [d, $^2J(\text{PP}) = 48$ Hz, RuP], 8.3 [d, $^2J(\text{PP}) = 48$ Hz, $^1J(\text{PtP}) = 3130$ Hz, PtP]. $\delta(^{13}\text{C}) = 204$ [2C, dm, $^3J(\text{PC}) = 21$ Hz, equatorial CO]; 222 [4C, m, $^1J(\text{PtC}) = 34$ Hz, axial CO]. If the reaction to form complex **4** is carried out in situ in CD_2Cl_2 , compound **5** is observed by ^{31}P NMR as a reaction intermediate.

[PtRuH(CO)₃(μ-dppm)₂][Cl] (5). [Pt(dppm)₂Cl₂] (30 mg, 0.028 mmol) and PPN[HRu(CO)₄] (22 mg, 0.029 mmol) were placed in an NMR tube and cooled to -80 °C. Deuterated methylene chloride (0.5 mL) was then added to the tube, resulting in the formation of an orange solution, which was allowed to slowly warm to room temperature. Compound **5** is stable in solution for several hours, but over longer periods it is transformed into **6** and **7**. Attempts to isolate solid samples of **5** resulted in mixtures of **6** and **7**. IR (CH_2Cl_2 solution): 2042 (m), 1988 (s), 1970 (sh). NMR in CD_2Cl_2 : $\delta(^1\text{H}) = -3.95$ [t, 1H, $^2J(\text{PH}) = 10$ Hz, $^1J(\text{PtH}) = 1270$ Hz, PtH]; 4.34 [m, 4H, $^3J(\text{PtH}) = 30$ Hz, PCH₂P]. $\delta(^{31}\text{P}) = 36.8$ [m, RuP]; 24.0 [m, $^1J(\text{PtP}) = 3260$, PtP]. $\delta(^{13}\text{C}) = 195.5$ [t, 1C, $^2J(\text{PC}) = 14$ Hz, $^2J(\text{PtC}) = 28$ Hz, CO anti to Pt]; 207.8 [t, 2C, $^2J(\text{PC}) = 13$ Hz, CO syn to Pt].

[PtRuHCl(CO)(μ-CO)(μ-dppm)₂] (6). [Pt(dppm)₂Cl₂] (100 mg, 0.096 mmol) was suspended in THF (50 mL). [PPN][HRu(CO)₄] (72 mg, 0.096 mmol) was dissolved in THF (20 mL) and added dropwise to the suspension over 30 min, resulting in a bright yellow solution and a white precipitate. The solvent was removed in vacuo, and the residue was extracted into THF (2 mL) and filtered. The solvent was removed from the filtrate in vacuo, and the residue was recrystallized from THF/Et₂O/pentane and dried in vacuo. Yield: 111 mg. The sample contained small amounts of a second compound, which was shown to be [PtRu(Cl)₂(CO)₂(μ-dppm)₂] (**7**). IR: $\nu(\text{CO}) = 1880$ sb, 1770 mb. NMR in CD_2Cl_2 : $\delta(^1\text{H}) = -5.45$ [tt, 1H, $^2J(\text{HPtP}) = 16$ Hz, $^3J(\text{HPtRuP}) = 3$ Hz, $^1J(\text{HPt}) = 1050$ Hz, PtH]; 4.23 (m, 1H, CH₂); 3.88 [m, 1H, $^3J(\text{PtH}) = 70$ Hz, CH₂]. $\delta(^{31}\text{P}) = 38.0$ [m, RuP]; 17.8 [m, $^1J(\text{PtP}) = 2940$ Hz, PtP]. $\delta(^{13}\text{C}) = 207.7$ [m, 1C]; 225.1 [m, 1C].

[PtRuCl₂(CO)₂(dppm)₂] (7). PPN[HRu(CO)₄] (72 mg, 0.096 mmol) was dissolved in CH_2Cl_2 (15 mL), and the solution was cooled to -80 °C. This solution was then added to [Pt(dppm)₂Cl₂] (100 mg, 0.096 mmol) in CH_2Cl_2 (15 mL) also at -80 °C, resulting in the formation of an orange solution. The solution was allowed to gradually warm to room temperature and then stirred for 4 days. The solvent was then removed in vacuo,

the residue was separated by chromatography (silica gel, CH_2Cl_2 /acetone 50:50), and the yellow band was isolated. The solvent was removed in vacuo, and the residue was recrystallized from CH_2Cl_2 /Et₂O. Yield: 85 mg, 74%. Anal. Calcd for $\text{C}_{52}\text{H}_{44}\text{Cl}_2\text{O}_2\text{P}_4\text{PtRu}$: C, 52.40; H, 3.72; Cl, 5.95. Found: C, 52.35; H, 3.71; Cl, 5.81. IR: $\nu(\text{CO}) = 2025$ ss, 1945 ss, 1905 sb, 1792 mb. NMR in CD_2Cl_2 : $\delta(^1\text{H}) = 4.70$ [m, 2H, PCHHP]; 4.09 [m, 2H, PCHHP]. $\delta(^{31}\text{P}) = 24.3$ [m, RuP]; 11.6 [m, $^1J(\text{PtP}) = 3060$ Hz, PtP]. $\delta(^{13}\text{C}) = 208.0$ [t, $^2J(\text{PC}) = 11$ Hz, $^1J(\text{PtC}) = 117$ Hz]; 192.4 [m, $^2J(\text{PtC}) = 180$ Hz].

X-ray Structure Determinations. **[PtRu₂(CO)₅(μ-CO)(μ-dppm)₂] (4).** Crystals of **4** were grown by slow diffusion of pentane into a methylene chloride solution. A red crystal was mounted on a glass fiber. Data were collected at 100 K on a Nonius Kappa-CCD diffractometer using COLLECT (Nonius, 1998) software. The unit cell parameters were calculated and refined from the full data set. Crystal cell refinement and data reduction was carried out using the Nonius DENZO package. The data were scaled using SCALEPACK (Nonius, 1998), and no other absorption corrections were applied. The reflection data and systematic absences were consistent with the monoclinic space group $P2_1/n$. The SHELXTL 5.03 (Sheldrick, G. M., Madison, WI) program package was used to solve the structure by direct methods and successive difference Fourier. All non-hydrogen atoms were refined with anisotropic thermal parameters. The hydrogen atoms were calculated geometrically and rode on their respective carbon atoms. The largest residual electron density peak ($1.523 \text{ e}/\text{\AA}^3$) was associated with the platinum atom.

[PtRuCl₂(CO)(μ-CO)(μ-dppm)₂] (7a). Crystals of **7a**· $\text{CH}_2\text{Cl}_2 \cdot 1/2$ pentane were grown by slow diffusion of pentane into a methylene chloride solution. A crystal was mounted in a capillary tube. Data were collected and treated as above. Systematic absences were consistent with either Cc or $C2/c$, but the noncentrosymmetric choice (Cc) had a better combined-figure-of-merit. The choice was borne out by a successful solution of the structure. Of the two solvent molecules, the methylene chloride was well behaved, while the pentane was disordered. It was modeled by fixing the α and β C–C bond lengths. An extinction correction was applied, and the absolute structure parameter was refined to a value of 0.334. The largest residual electron density peak ($1.299 \text{ e}/\text{\AA}^3$) was associated with the pentane of solvation. The crystal data and refinement parameters are listed in Table 1. Selected interatomic distances and angles are listed in Table 3.

Acknowledgment. We thank the NSERC (Canada) and the PRF for financial support.

Supporting Information Available: Table of X-ray data in CIF format are available on the web only. This material is available free of charge via the Internet at <http://pubs.acs.org>.

OM990032Z